Int. J. Solids Structures Vol. 19, No. 5, pp. 393–410, 1983
Printed in Great Britain

0020-7683/83/050393-18$03.00/0
Pergamon Press Ltd

AN EXPERIMENTAL INVESTIGATION OF PASS BANDS AND STOP BANDS IN TWO PERIODIC PARTICULATE COMPOSITES†

VIKRAM K. KINRA
Aerospace Engineering Department, Texas A&M University, College Station, TX 77843, U.S.A.

and

ERIC L. KER
Department of Mechanical Engineering, University of Colorado, Boulder, CO 80309, U.S.A.

(*Received* 23 *June* 1982)

Abstract—An important property of the periodic composites is that the dispersion curve is characterized by pass bands and stop bands. In the past these have been demonstrated, analytically and experimentally, for layered and fibrous composites. The purpose of the present experimental investigation is to show that the same phenomena exist in periodic particulate composites.

1. INTRODUCTION

Composite materials differ from the homogeneous materials most markedly in their dynamic mechanical behavior, particularly when a characteristic length of the deformation becomes comparable to that of the microstructure. Therefore, from the viewpoint of engineering applications, an understanding of the dynamic response is important. Propagation of periodic and transient waves through composites has been the subject of numerous investigations (see [1] for a relatively recent review, see also [2]). An important characteristic of the propagation of periodic waves through periodic composites is the existence of pass bands and stop bands. These have been experimentally demonstrated in both the layered (one-dimensional) composites[3, 4] as well as the fibrous (two-dimensional) composites[5, 6]. To the best of our knowledge, similar results, either theoretical or experimental, have not been reported for the three-dimensional case of periodic particulate composites; this is the purpose of the present work.

The phase velocity of longitudinal waves through periodic particulate composites was measured as a function of frequency. Two composites were studied: (1) Glass spheres in an epoxy matrix and; (2) Steel spheres in a PMMA matrix. Two pass bands were observed in the first composite, whereas three pass bands could be identified in the second. The experimental technique employed was that of through-transmission of an ultrasonic pulse.

2. SPECIMEN PREPARATION

2.1 *Glass-epoxy composite*

Glass spheres of 2 mm dia. were arranged in a primitive (or simple) cubic lattice with a unit cell of $(2.54\ \text{mm})^3$ dimensions. An aluminum mold, 25.4×25.4 mm, was fabricated by drilling 1.5 mm dia. $\times$ 3 mm deep bores in an 8×8 square array. Each square measured 2.54×2.54 mm. The desired negative image of the mold was produced by pouring an epoxy[7] into the mold. When cured and detached the epoxy layer contained 3 mm long cylindrical protrusions; the space between the protrusions is a lattice site. One sphere was manually placed in each of the sixty-four lattice sites. The assemblage was inserted into a second mold, the epoxy was poured and degassed for a long period of time to insure that all the trapped air was evacuated, and the curing cycle was repeated. The detached sheet was machined on both sides to a thickness of 2.54 mm with glass spheres at the center of the thickness direction. Ten layers were produced in this manner, a thin layer of the epoxy was used to join them together, the assemblage was inserted into another suitable mold, and the curing process was repeated under a suitably high pressure. The faces of the specimen were lapped and polished to a 20 μm finish. The overall dimensions of the specimen were $(25.4\ \text{mm})^3$.

†This paper is dedicated to Prof. H. Kolsky on his sixty-sixth birthday.

Table 1. Acoustic properties of the materials

Material	C_1 (mm/μs)	C_2 (mm/μs)	ρ	ν	m (nepers/mm-MHz)
Epoxy	2.54	1.16	1.18	0.370	0.045
Glass	5.28	3.24	2.492	0.200	negligible
PMMA	2.63	1.32	1.16	0.334	0.02
Steel	5.94	3.22	7.8	0.292	negligible
Polystyrene	2.33	1.12	1.15	0.350	0.006

Table 2. Geometric properties of the composites

Composite	Inclusion Radius a (mm)	Unit Cell (Dimensions in mm)	d (mm)	$\tilde{C}$(%)
Glass/Epoxy	1	Primitive Cubic (2.54^3)	2.54	25.6
Steel/PMMA	0.55	Primitive Tetragonal (1.32 × 1.32 × 2.63)	2.63	15.2

The acoustic properties of the constituents are listed in Table 1, while the geometric properties of the composite are given in Table 2. In Table 1, C_1 and C_2 are, respectively, the longitudinal and shear wavespeeds, ρ is the density, ν is the Poisson's ratio, and m is given by $\alpha = mn$, where α is the attenuation and n is the frequency. In Table 2, a is the inclusion radius, d is the unit cell dimension in the direction of wave propagation, and $\tilde{C}$ is the volume fraction of inclusions.

2.2 *Steel—PMMA composite*

It was considered desirable to obtain mutually corroborating results with two composites with different acoustical properties. Epoxy was found to be a fairly attenuative material. To reduce attenuation the matrix material was changed to PMMA[8]. Steel has substantially higher stiffness and density as compared to glass; see Table 1. Therefore, the inclusion material was changed to steel[12]. Thus the acoustical conditions obtaining in these two composites are significantly different. Further, for reasons that will become clear later on, the inclusion diameter was reduced from 2 mm to 1.1 mm. From symmetry considerations it is desirable to use the primitive cubic unit cell. However, for the desired 2.63 mm dimension in the wave propagation direction (the reason for this is given below), this would have resulted in a volume fraction $\tilde{C} = 0.037$. In the absence of any theoretical results even remotely similar to the problem under consideration on the basis of which one could design the experiment, it appeared that for this low $\tilde{C}$, the scattering effects may be too small to be detected with an acceptable signal-to-noise ratio. This is the reason for choosing a primitive tetragonal unit cell of dimensions $1.32 \times 1.32 \times 2.63$ mm with the largest dimension in the direction of wave propagation: then $\tilde{C} = 0.152$.

For the case of one-dimensional layered composites, Lee and Yang[18] have shown that the stop bands correspond to the following geometric condition: twice the unit cell dimension equals an integral multiple of the wavelength of the periodic wave in the composite. In terms of a properly normalized wavenumber, ξ, this condition may be written as $\xi = m$, where $\xi = \langle k_1 \rangle d/\pi$, m is a positive integer, d is the demension of the unit cell in the direction of wave propagation, k is the wave number, the subscripts $(\ )_1$ and $(\ )_2$ denote, respectively, the longitudinal and the shear disturbances, and $\langle\ \rangle$ denotes a composite property (ensemble average). Only for design purposes we assumed that the corresponding criterion for a periodic *particulate* composite is not too different from $\xi = m$. Further, it is desirable to have the

(postulated) cut-off frequencies coincide with the center-frequencies of the crystals (0.25, 0.5, 1.0 and 2.0 MHz). In order for the first cut-off to occur near 0.5 MHz, d should be 2.63 mm. (Same reason led to $d = 2.54$ mm for the glass-epoxy composite.)

The mold consisted of a 31.75 mm (1.25 in.) steel cylinder with 0.5 mm dia. bores drilled in a 1.32×1.32 mm square array, and two alignment pins near the edges. One steel ball was manually placed in each of the 314 holes. The mold was placed in a Beuhler Specimen Mounting Press[8], the desired amount of PMMA powder was accurately weighed and poured into the mold and subjected to a pressure of 35 MPa (5000 psi) at 190° C (375° F) for 10 min. When the disk is removed from the mold, it has steel balls protruding from the surface (it also has two alignment holes near the periphery). Hence, the disk was pressed against a flat surface and the molding process was repeated. A photograph of a single disk is shown in Fig. 2. Several disks were produced in this manner. The desired number of disks (5 or 10) were stacked together, two steel pins were threaded through the alignment holes in each of the disks, and the assemblage was taken through another cycle of molding process. The steel pins were left in place. Since these pins are always outside the circular area illuminated by the ultrasonic beam, they do not interfere with the measurement. The final lengths of the 5- and 10-layer specimens are 13.15 and 26.3 mm respectively. An end view photograph of the 5-layer composite is also shown in Fig. 2. From the top half of Fig. 2 it is apparent that there are some variations in the interparticle distances within the layer. These are a result of the corresponding variations in the steel mold. It is emphasized that these variations are *systematically* communicated to each of the layers. Hence, in the direction of wave propagation (which is the important direction in the present instance) the periodicity is exact, in the transverse directions, the periodicity suffers from the variations under discussion.

The acoustic properties of the constituent materials are listed in Table 1 while the geometric properties of the composite are given in Table 2.

Two *random* particulate composites were also prepared; these were identical to the two *periodic* composites described above in all other respects. Exactly the same preparation procedure was followed with only one difference. Instead of the periodic mold, a flat-surfaced mold was used, the PMMA powder was poured first and the steel balls were sprinkled next. This minimized the clustering of the steel balls. Also, upon falling the balls got trapped in the PMMA powder, producing the desired randomness. We note that in the axial direction the composite is periodic. In [9, 17] this potential source of error was systematically examined. Since specimens used in [9, 17] were orthorhombic in shape, $\langle C_1 \rangle$ could be measured in three perpendicular directions and was found to be nearly the same. In this work, due to the cylindrical shape of the specimen, it is not possible to measure $\langle C_1 \rangle$ normal to the axis, hence, we are forced to assume that the composite behaves in a random manner. In view of the incoherent nature of the scattering of the incident wave by the particles within each layer and the results of [9, 17], it appears to be a reasonable assumption.

3. EXPERIMENTAL PROCEDURES

3.1 *Apparatus*

Two types of ultrasonic through-transmission apparatuses were used in this investigation: (1) water immersion apparatus and (2) direct contact apparatus. A detailed description of the first may be found in [9]. The principal drawback of this technique is that a significant amount of energy is lost at the pair of water-specimen interfaces, hence the need for the direct contact apparatus described next.

A schematic of the direct contact apparatus is shown in Fig. 1. The experiment is initiated by a pulse from the Time Mark Generator (Tek. TM 184) which simultaneously triggers a Pulse Generator (Tek. PG 501) and the oscilloscope. Arbitrarily, this time is taken as $t = 0$. The Pulse Generator/Function Generator (either Tek. FG 502 or Wavetek Model 164)/RF Amplifier (EIN Model A 150) combination is used to produce a toneburst of the desired duration (5–50 μs), frequency ($0.2 \leqq n \leqq 2.5$ MHz), and amplitude (about 300 V peak-to-peak). The electrical signal is applied to one of a pair of accurately matched ultrasonic transducers which acts as the transmitter, the other is used as the receiver. The nominal center-frequencies of these crystals are 0.25, 0.5, 1.0 and 2.0 MHz. The last three were obtained from the vendors[10], the first ones (0.25 MHz) were home-made. Here, X-cut ceramic (PZT-5) plates (25.4×25.4 mm) were obtained from[11]. The well-known problem of ringing was minimized by a heavy acoustic

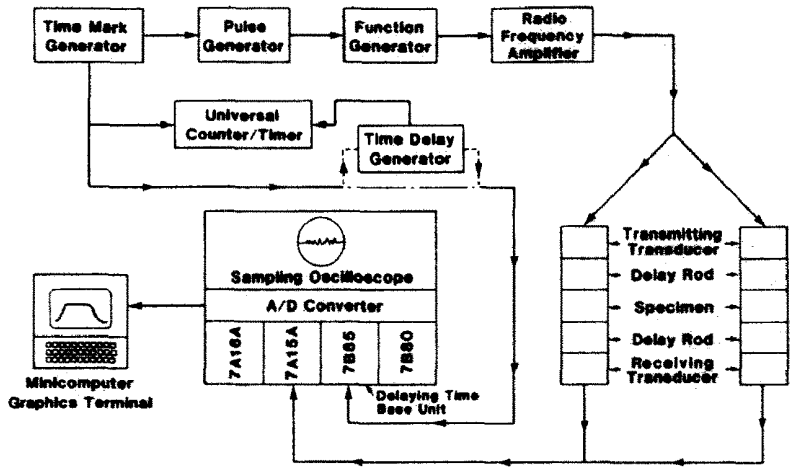

Fig. 1. A schematic of the apparatus.

loading of the back of the crystal; an epoxy saturated with fine tungsten powder was used for this purpose. However, in the early stages of this work the domestic transducer suffered from a problem not encountered in the commercially made transducers. The problem stems from the fact that the attenuation in the tungsten/epoxy backing material (which may be viewed as a random particulate composite) is rather small at 0.25 MHz. In the case of the receiver (the same argument applies to the transmitter), when the incident toneburst in polystyrene strikes the crystal, a significant fraction of the energy is propagated into the backing. If the attenuation had been sufficiently large, this energy would have been completely absorbed in the backing material. As it is, a part of this energy is reflected at the rear face of the backing, reappears at the crystal, and interferes with the measurement. This problem was circumvented by using an unusually long (70 mm) backing. The twice-transit-time in the backing was found to be about 60 μs. Since the duration of a typical toneburst at these frequencies is about 50 μs, measurements could be made prior to the arrival of this spurious reflection.

A pair of polystyrene delay rods ($50.8 \times 50.8 \times 25$ to 100 mm long) was inserted between the specimen and the transducers. Since the acoustic impedance of the polystyrene and PMMA is very nearly equal, the reflection at a polystyrene/PMMA interface is negligibly small, and all of the wave is transmitted, see Table 1. A thin layer of castor oil was used to bond the transducers to the delay rods. In order to obtain a reproducible layer thickness from one test to another, the transducer holders were axially compressed to a constant load of about 100 N (20 lbf) with the help of a spring-loaded screw mechanism. The coupling between the delay rods and the specimen, on the other hand, was desired to be acoustically rigid; a low melting compound (65° C), namely, phenylsalicylate was used for this purpose. Its use permitted quick and easy debonding and rebonding.

The signal received through the composite is monitored on a Tek. 7704 A oscilloscope equipped with a P7001 Processor (A/D converter), two 7A16A amplifiers, a 7B80 Time Base Unit and a 7B85 Delaying Time Base Unit. Whenever it is desired to carry out a spectroscopic analysis of the data, the digitized waveform is transferred from the P7001 Processor to a desk top microprocessor (Tek. 4051 smart graphics terminal). The upper trace of the oscilloscope is triggered at time $t = 0$; the lower trace, on which the received waveform is displayed, is triggered after a suitable time delay and swept at a very fast rate (typically 100 ns/division) to permit a detailed examination of the waveform. The 7B85 is used for this purpose and the delay time is obtained to an accuracy of 10 ns. Whenever higher accuracy is desired, the time delay is generated externally and measured with the help of a Universal Counter/Timer (Teletronix DC 505 A) which has an accuracy of about 5 ns; this path is shown in dotted lines. To obtain a continuous display, the experiment is repeated at a rate of about 1 KHz. Finally, depending upon convenience, the two apparatuses were used interchangeably. Frequently, both apparatuses were used for the same measurement to produce redundant data that were checked against each other.

3.2 *Measurement techniques*

Toneburst method. In this method the phase velocity of longitudinal wave, $\langle C_l \rangle$ is determined by measuring the flight time of a toneburst through two specimens of known thicknesses; typical incident and transmitted tonebursts are shown in Figs. 8 and 9. Since we are concerned with phase, rather than group, velocity, all measurements are made with a *reference peak* near the middle of the toneburst which typically contains twenty cycles. Let t be the delay time required to make the reference peak coincide with (say) the center graticule of the screen. Let t_1 and t_2 be the delay times and A_1 and A_2 be the amplitudes of the received signal at the reference peak for specimens of thickness W_1 and W_2, respectively. Then

$$\langle C_l \rangle = (W_2 - W_1)/(t_2 - t_1) \tag{1}$$

and

$$\langle \alpha \rangle = \ln(A_1/A_2)/(W_2 - W_1). \tag{2}$$

Note that identical delay rods are used for both specimens. Occasionally, when the frequency is high and, therefore, the attenuation is large, the received signal through the thicker specimen may be too small to be measured satisfactorily. When this happens only one specimen is used for $\langle C_l \rangle$ measurement. The thicker specimen is replaced by the pair of polystyrene delay rods joined together with a phenylsalicylate bond. The attenuation, however, is always measured by using two specimens.

This procedure of obtaining $\langle C_l \rangle$ and $\langle \alpha \rangle$ through a comparative measurement eliminates the transit time through the delay rods as well as the errors due to the following sources: (1) inherent time delays in various pieces of electronic equipment; (2) transit time through castor oil layers and phenylsalicylate bonds; and (3) the transducer characteristics.

Frequently, redundant measurements of $\langle C_l \rangle$ were obtained by treating all the peaks of a toneburst as the reference peaks. Expectedly, $\langle C_l \rangle$ fluctuated somewhat when the reference peak was near the head of the pulse. However, $\langle C_l \rangle$ rapidly attained a constant value (within the 1% error of measurement) as the peak number of the reference peak increased, i.e. as the reference peak became increasingly farther from the head of the pulse. This reassured us that we are measuring the phase rather than the group velocity.

Error analysis. A systematic error analysis of the measurement procedures was reported in [9] for the water-immersion apparatus, and in [25] for the direct-contact as well as the water-immersion apparatus. A detailed discussion of some of the modelling errors may be found in [17]. Here, we merely report the results of these calculations. The measurement error in $\langle C_l \rangle$ is estimated to be 1%. It is more difficult to assign a single number to the error estimate in $\langle \alpha \rangle$; see [27]. It ranged from about 1% for the "best" case to about 10% for the "worst" case. We make the conservative claim that the measurements are accurate to about 15%. These estimates were amply borne out by the reproducibility of the experimental results.

Ultrasonic spectroscopy. The toneburst method is quite accurate but also very time consuming. A more efficient though somewhat less accurate method is that of ultrasonic spectroscopy. Unlike the toneburst method where a nearly monochromatic signal is applied to the transmitter, here a short duration (200 ns–2 μs) spike is used. The resulting P-wave has a broad range of frequencies. The propagation of this transient waveform through the composite is studied in terms of its constituent Fourier components. For two specimens of thickness W_1 and W_2, let $a_1(t)$ and $a_2(t)$ be the received time-domain signals, and t_1 and t_2 be the delay times, respectively. Let A_1^* and A_2^* be the Fourier transforms of $a_1(t)$ and $a_2(t)$, respectively. Let $A_1 = |A_1^*|$, $A_2 = |A_2^*|$, ϕ_1 = phase of A_1^*, ϕ_2 = phase of A_2^*, $\phi = \phi_1 - \phi_2$, and $t = t_1 - t_2$. A straightforward calculation yields

$$\langle \alpha(\omega) \rangle = \ln(A_1/A_2)/(W_2 - W_1), \tag{3}$$

and

$$\langle C_l(\omega) \rangle = (W_2 - W_1)/(t + \phi/\omega), \tag{4}$$

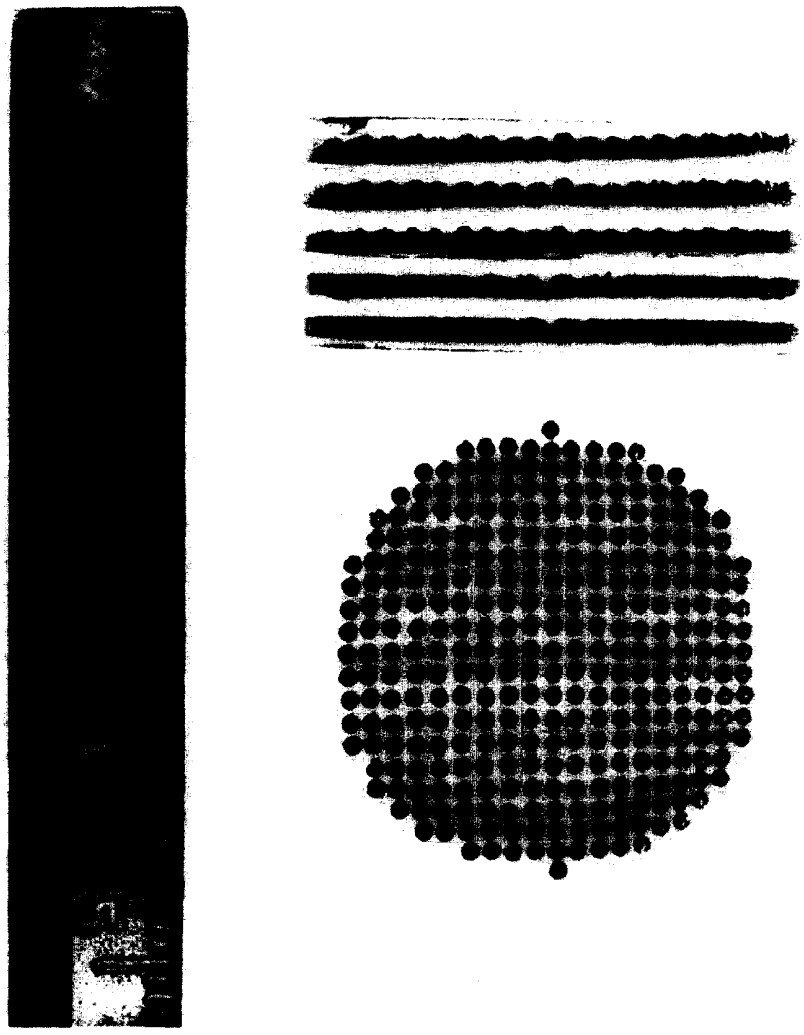

Fig. 2. Two photographic views of the steel/PMMA periodic particulate composite. The direction of wave propagation is along the axis of the cylinder. Unit cell: $1.32 \times 1.32 \times 2.63$ mm.

where ω is the circular frequency; $\omega = 2\pi n$. With reference to Fig. 1, the transient waveform ($a_1(t)$ or $a_2(t)$) is digitized by P7001 Processor, the data is transferred to the Tek. 4051 Graphics Terminal where a standard FFT routine is used to calculate the Fourier transforms (Tek. 4051 R08 SPS Rom Pack #2) and $\langle\alpha\rangle$ is computed by eqn (3). Although this method has in the past been successfully used to measure $\langle C_1\rangle$ for homogeneous materials (aluminum, polystyrene, steel, etc.)[24], and *random* particulate composite[25], which, in the aggregate, behave in an isotropic homogeneous manner at long wavelengths, it could not be used for the present case of a *periodic* composite and the reason for this is considered worth mentioning. The value of ϕ that can be obtained from the Fourier transform is non-unique up to integral multiples of 2π. If it is known *a priori* that the dispersion curve, $\langle C_1\rangle$ vs ω, is continuous (e.g. homogeneous materials), then the non-uniqueness in ϕ presents no problem. One starts with some frequency where the behavior of $\langle C_1(\omega)\rangle$ is known (e.g. the long-wavelength limit for the case of random particulate composites[25]) and follows $\langle C_1\rangle$ as ω is gradually varied. If the value of ϕ computed by the FFT takes a jump of an integral multiple of 2π, so does $\langle C_1\rangle$. Since $\langle C_1(\omega)\rangle$ is known *a priori* to be continuous, the jump in $\langle C_1\rangle$ can be eliminated by removing the spurious multiples of 2π from ϕ. If, on the other hand, it is known *a priori* that the dispersion curve is *discontinuous*, as is the case here (see Figs. 3–5), then this procedure cannot be used with confidence. Across the discontinuity in $\langle C_1\rangle$, the phase ϕ will also suffer from a corresponding jump discontinuity, see eqn (4). (In our experiments, this jump in ϕ was found to be about 30 radians.) Since ϕ, as computed by the FFT, is non-unique up to an integral multiple

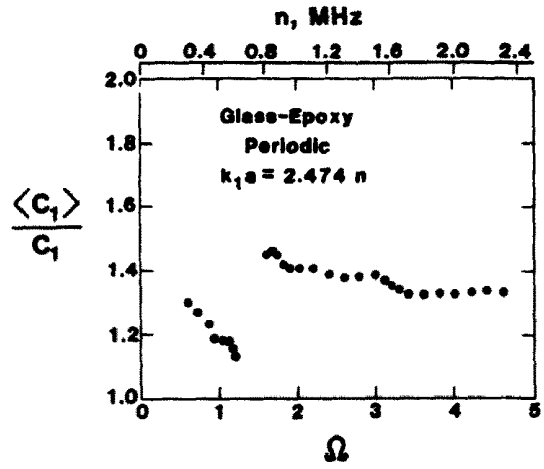

Fig. 3. The dispersion curve for the glass/epoxy periodic composite has one stop band and two pass bands.

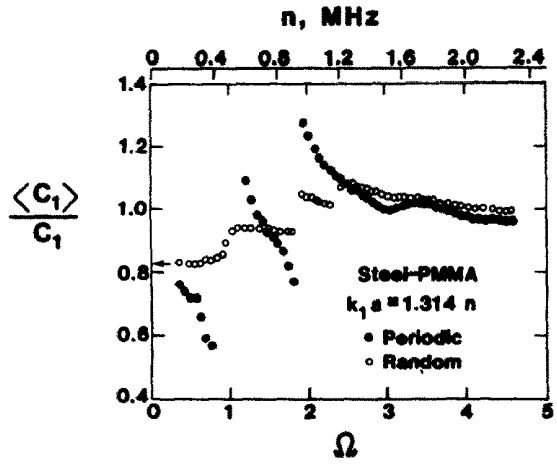

Fig. 4. The dispersion curve for the steel/PMMA periodic composite has two stop bands and three pass bands. For the random case it has three discontinuities. The arrow at $\langle C_1\rangle/C_1 = 0.83$ is the long-wavelength analysis of [16] for the random case.

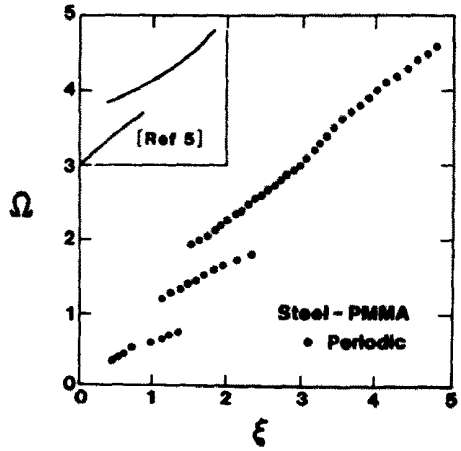

Fig. 5. Normalized frequency vs wavenumber for steel/PMMA periodic composite. The pass bands overlap. For pure matrix, $\Omega = \xi$. Upper left: data from [5] for a fibrous composite; data have been shifted by 3.0 along Ω-axis.

of 2π, the jump in ϕ (corresponding to the jump in $\langle C_1 \rangle$) cannot be uniquely determined. Of course, with experience and by examining the limits of the two dispersion branches on either side of the jump (Figs. 3 and 4), one can make a fairly good guess at the integral multiples of 2π missing from the phase information. However, such a procedure is at best a fudge device and was deemed unacceptable, particularly because the main objective of this paper is the determination of the jump in $\langle C_1 \rangle$ across a no-pass band. Therefore, all the $\langle C_1 \rangle$ data reported in this work was obtained with the toneburst method described in Section 3.2. The attenuation $\langle \alpha \rangle$, on the other hand, was measured by using both techniques, wherever possible.

4. RESULTS

4.1 *Properties of the constituents*

Several specimens of epoxy, PMMA, and polystyrene were prepared with thickness ranging from about 15–100 mm. C_1 and C_2 were measured over the frequency range of 0.25–5 MHz at room temperature, and were found to be frequency-independent, within the errors of measurement. Since thicker specimens were used, these measurements are accurate to about $\pm 0.5\%$. The attenuation α was found to increase linearly with n: $\alpha = mn$. The measured values of the material properties are listed in Table 1. The properties for glass[20] and steel[12] are taken from the manufacturer's specifications, and are assumed to be frequency-independent.

It is well-known that the acoustic properties of polymeric materials are sensitive to temperature. To minimize the effect of this source of error, all measurements were made at the same temperature of 22 ± 1°C. For PMMA, a 1°C change in temperature will cause (roughly) no more than 0.1% change in C_1 [26]; this may be considered negligibly small in view of the 1% measurement error. Next, the longitudinal attenuation of PMMA at 22°C and 1 MHz frequency is 0.02 nepers/mm, see Table 1. A 1°C change in temperature will cause (roughly) a 0.00035 nepers/mm change in the attenuation which may be safely neglected.

4.2 *Velocity measurements*

Throughout this work, wave propagation was made to occur along one of the symmetry axes. For glass/epoxy composite, with a primitive cubic unit cell, all three axes are equivalent. For the steel/PMMA composite, with a primitive tetragonal unit cell, the direction of propagation is along the larger dimension, $d = 2.63$ mm.

We introduce a normalized frequency $\Omega = k_1 d/\pi (= 2d/\lambda_1 = 2dn/C_1)$, where λ is the wavelength. Furthermore, the unprimed and primed quantities, ( ) and ( )′, refer to the matrix and the inclusion properties, respectively. For example, λ_1 is the longitudinal wavelength in the matrix material. Physically, when $\Omega = 1$, the wavelength in the *matrix* equals twice the length of the unit cell. The toneburst method was used for velocity measurements. The phase velocity as a function of n (or Ω) is shown in Figs. 3 and 4. Now, for a layered composite a stop band implies the range of frequencies over which the composite completely reflects all of the incident wave and there is no transmission. For the periodic particulate composites no such frequencies were found; a finite signal was received at all frequencies. Therefore, in the context of the present experiments the expression "stop band" will be used to denote that range of frequencies over which velocity could not be measured (see Section 4.6) and across which $\langle C_1 \rangle$ takes a finite *positive* jump with increasing frequency (n); the latter is a characteristic of both layered and fibrous composites.

The glass/epoxy composite exhibits one stop band and two pass bands; the steel/PMMA composite reveals two stop bands and three pass bands. Consistent with the earlier observations for layered[3, 4] and fibrous[5, 6] composites, $\langle C_1 \rangle$ decreases with Ω in each pass band.

A solution for the case of a periodic particulate composite has not yet been reported. However, an exact solution for the case of periodic wave propagation through periodic *layered* composite is available[1–3]. It has been shown that at the stop band (or cut-off), the *effective wavenumber* in the composite satisfies the condition $\xi = \langle k_1 \rangle d/\pi = m$, where m is a positive integer. This condition is approximately satisfied by the stop bands observed in Figs. 3 and 4 (this will be explained in the next subsection).

Within the range of frequencies tested, namely, $0.3 \leqq n \leqq 2.05$ MHz for glass composite and $0.17 \leqq n \leqq 2.3$ MHz for the steel composite, the criterion $\xi = m$ predicts additional second and third stop bands at $n = 1.4$ MHz ($\xi = 2$) and $n = 2.0$ MHz ($\xi = 3$), respectively, for the glass

composite; for the steel composite additional stop bands at $n = 1.5$ MHz ($\xi = 3$) and $n = 1.9$ MHz ($\xi = 4$) are predicted; none of these bands is observed. In fact, $\langle C_1 \rangle$ varies continuously with n across the anticipated stopbands.

The following is offered as a plausible explanation for the absence of the higher stop bands. In addition to d—the length of the unit cell in the direction of wave propagation—there is a second characteristic length associated with this problem, namely, the radius of the *spherical* inclusion, a. Owing to its simple geometry, an elastic sphere embedded in an elastic matrix is capable of sustaining resonances. These have been studied by Flax and Überall[13] who showed that for the case of an iron sphere in an aluminum matrix, these resonances occur when $k_1 a = 0(1)$. Another manifestation of the particle resonance is the existence of peaks in the γ_N vs $k_1 a$ curves, where γ_N is the total scattering cross-section of a sphere; see Appendix H of[14]. Here again the effect is pronounced when $k_1 a = 0(1)$. In their experiments with *random* particulate composites (i.e. an aggregate of elastic scatterers) consisting of lead spheres in an epoxy matrix, Kinra *et al.*[15] showed that the influence of particle resonance on $\langle C_1 \rangle$ was significant when $k_1 a = 0(1)$. Similarly, the influence of particle resonance on the attenuation, $\langle \alpha \rangle$, has also been recorded experimentally[28]. Thus it is fairly well established that when the wavelength becomes comparable to the inclusion size, i.e. $ka = 0(1)$, particle resonances are excited, and that this phenomenon measurably affects the wave propagation behavior of the composite. For the present case of the glass/epoxy composite, $k_1 a = 2.474\, n$; see Tables 1 and 2. The range of frequencies tested is $0.3 \leqq n \leqq 2.05$ MHz and, therefore, $k_1 a$ varies in the range $0.75 \leqq k_1 a \leqq 5$. The point is that $k_1 a$ is in the correct range for the excitation of particle resonances to occur. We now postulate that these resonances are, in fact, excited in our experiments. Furthermore, for the case of a layered composite, Lee and Yang[18] have shown that at the frequencies corresponding to the ends of the stop bands, "... the Floquet waves ... are simply normal modes of oscillation of the system, all elements moving in phase. There is no propagation, and in conformity with this circumstance, the group velocity at the ends of the bands... is zero." Thus there are two resonance effects in the present experiments: the lattice resonances and the particle resonances. We now offer the conjecture that for the glass/epoxy composite under consideration in the first stop band ($m = 1$, wavelength is $2d$ and, therefore, large compared to a) the lattice resonance effects dominate the particle resonance effects. On the other hand, in the second stop band ($m = 2$, wavelength is d and hence comparable to a), the reverse is true, i.e. the particle resonance effects dominate the lattice resonance effects, thereby masking the second stop band.

We now mention a *specific* resonance mode which *may be* responsible for masking the higher stop bands: *this mode has to do with the rigid-body rectilinear translation of a single sphere in an unbounded matrix*[29]. Kinra and Anand[17] have experimentally studied wave propagation through a glass-epoxy (same constituents as used in this investigation) *random* particulate composite. The wave propagation was found to occur along two separate branches: at long-wavelengths along the *acoustical branch*; and at short-wavelengths along the *optical branch*. Following the analysis of Moon and Mow[29], they attributed the transition to the rigid-body resonance mode mentioned above. This transition occurred in the range $2.5 \leqq k_1 a \leqq 3.75$ (approximate empirical limits), i.e. $2 \leqq \Omega \leqq 3$. Taking $\langle C_1 \rangle / C_1 = 1.4$ over $2 \leqq \Omega \leqq 3$ (Fig. 3), the transition occurs over $1.4 \leqq \xi \leqq 2.1$, i.e. if the spheres had been distributed in a random homogeneous manner, the wave propagation would have occurred along the optical branch for $\xi \geqq 2$. This may very well be the reason for not observing the second ($\xi = 2$) and the third ($\xi = 3$) stop bands.

Another plausible reason is the matrix attenuation. It is well known that the attenuation of these polymers, when expressed as nepers/wavelength, is nearly constant. At a stop band, $\xi = m$, there are $m/2$ wavelengths in each unit cell. Since the phenomenon of cut-off is due to interference of multiply-reflected waves, the matrix attenuation will become more important at higher stop bands. However, in view of the rather small matrix attenuation (see Table 1), it is believed that this is less likely a reason than the particle resonance.

The glass/epoxy composite was tested first. It is for the purpose of testing the validity of the plausible explanations given above that the steel/PMMA composite was designed and tested next. The diameter of the steel spheres was chosen to be 1.1 mm—roughly half of the glass spheres. For glass $a/d = 0.394$, for steel $a/d = 0.209$. Thus, for the same value of Ω in both

specimens, k_1a is roughly one-half for the steel specimen. The excitation of the particle resonance—if it is indeed the reason for masking the higher stop bands in the glass composite—should be postponed along the Ω axis for the steel composite, thereby revealing additional stop bands. Furthermore, for sufficiently high values of Ω (hence, of k_1a), the higher pass bands should be masked even in the steel specimen. Both of these conjectures are borne out by the data in Fig. 4. For the steel specimen $k_1a = 1.314\ n$, $0.17 \leqq n \leqq 2.3$ MHz is the range of frequencies tested, hence $0.22 \leqq k_1a \leqq 3.02$ (for the glass specimen $0.75 \leqq k_1a \leqq 5.0$). The steel/PMMA data reveal one extra stop band, corresponding to $\xi = 2$. Two higher stop bands corresponding to $\xi = 3$ ($n = 1.5$ MHz, $k_1a = 1.97$) and $\xi = 4$ ($n = 1.9$ MHz, $k_1a = 2.5$) are not observed. These observations support our conjecture that the particle resonance is the reason for not observing the higher stop bands.

4.3 *Frequency-wavenumber plot*

When the dispersion data for the periodic steel composite is recast in the form of a normalized frequency vs a normalized wavenumber plot, it reveals an interesting phenomenon which is absent in the case of a periodic *layered* composite. First, we briefly summarize the corresponding results obtained with a layered composite. With reference to Figs. 1–3 of Ref. [3], the frequency-wavenumber plot for a layered composite has the following characteristics. Along the ξ-axis the first branch of wave propagation (frequently called the acoustical branch) terminates at $\xi = 1$. The second branch (frequently called the first optical branch) starts at $\xi = 1$ and terminates at $\xi = 2$, and so on. The important point is that along the ξ-axis the two branches do not overlap. In the following we show that the corresponding branches for a periodic *particulate* composite do overlap.

Ω vs ξ for the periodic steel composite is shown in Fig. 5. The first and the second pass bands overlap over $1.1 < \xi < 1.25$; the second and the third pass bands overlap over $1.5 < \xi < 2.4$. The interesting conclusion is that the same effective wavenumber (or wavelength) can be produced by two different frequencies. The first and the second stop bands satisfy the condition $\xi = 1$ and $\xi = 2$ (which are exact only for a layered composite) only in an approximate sense. It has been previously suggested [1, 3] that for the layered composites the Ω-ξ plot in various pass bands should lie along a single straight line. Herrmann *et al.* [23] showed analytically that this is incorrect; in Fig. 5 one may see an experimental verification of the preceding statement for the case of particulate composites. In particular, at low Ω the data approaches $\Omega \cong 0.8\ \xi$ whereas at high Ω, it approaches $\Omega \cong 0.96\ \xi$ (see also Fig. 4).

When the glass/epoxy data is recast into a similar Ω-ξ plot (which has been omitted for brevity) the first stop band also satisfies the condition $\xi = 1$ only approximately. At the two ends of the stop band $n = 0.6$ MHz, $\xi = 1.06$; and $n = 0.8$ MHz, $\xi = 1.10$. The two pass bands do not overlap in this case. Finally, the dispersion curve for the pure matrix would be the straight line $\Omega = \xi$.

Having observed that for particulate composites the pass bands overlap, we reexamined the experimental results of Sutherland and Lingle [5] to see if the same phenomenon also exists in fibrous composites. Although they failed to notice it, we will show in the following that their pass bands also overlap. They considered harmonic wave propagation (normal to the fibers) in a periodic composite consisting of tungsten fibers in an aluminum matrix. Their data for the case of 2.2% volume fraction of tungsten—when properly normalized and recast into an Ω-ξ plot—is also shown in Fig. 5. Note that for clarity the data have been shifted by 3.0 along the Ω-axis. Consistent with our results, the two pass bands overlap in $0.39 \leqq \xi \leqq 0.85$. Furthermore, the condition $\xi = 1$ for the first stop band (in a layered composite) is satisfied only in an approximate sense. The first pass band is: $0.13 \leqq \Omega \leqq 0.72$, $0.14 \leqq \xi \leqq 0.85$; the second pass band is: $0.81 \leqq \Omega \leqq 1.74$, $0.39 \leqq \xi \leqq 1.77$. For the case of 22.1% volume fraction of tungsten fibers they observed only the first band. Hence, a comparison could not be made.

4.4 *Comparison of random and periodic dispersion data*

As described in Section 3, Experimental Procedures, two steel/PMMA composite specimens were fabricated in which the spheres were distributed in a random homogeneous manner, otherwise these specimens were exactly identical to the periodic specimens in all respects: volume fraction, inclusion radius, and overall size. The objective was that a comparison of

equivalent periodic and random composites would clearly bring out the influence of lattice periodicity on the overall wave propagation behavior. The dispersion data for the random case is also plotted in Fig. 4. In the following the subscripts $(\ )_P$ and $(\ )_R$ will be used to denote periodic and random composites, respectively. At low frequencies $\langle C_{1R}\rangle$ agrees remarkably well with the results of a long-wavelength analysis by Datta[16] which predicts $\langle C_{1R}\rangle/C_1 = 0.83$. This is indicated by an arrow on the $\langle C_1\rangle/C_1$ axis. This analysis rests on the assumption that $ka \ll 1$, where k is any one of the four possible wavenumbers k_1, k_2, k_1', and k_2', and a is the inclusion radius. It is also interesting to note that in the low frequency limit $\langle C_{1P}\rangle$ and $\langle C_{1R}\rangle$ appear to be converging to nearly equal limits. Heuristically, when the wavelength becomes very large compared to the scale of the microstructure, the difference in the wave motion for the two cases should become small. As n increases the two dispersion curves diverge rapidly and substantially. This is one clear manifestation of the lattice periodicity. Furthermore, $\langle C_{1R}\rangle$ registers three fairly discrete increases at 0.45 MHz ($k_1a = 0.6$), 0.9 MHz ($k_1a = 1.2$) and 1.15 MHz ($k_1a = 1.5$). For $n > 1.2$ MHz, $\langle C_{1R}\rangle$ decreases slowly and appears to reach a high frequency limit of about 1.0 which is about 20% larger than its low frequency limit. In going from low frequency regime to high frequency regime, an increase in $\langle C_1\rangle$ in random particulate composites has also been observed previously for glass/epoxy[17] and lead/epoxy[15] composites, where it was conjectured that this increase is due to the excitation of the resonances of the spherical inclusions. Another interesting observation is that at high frequencies the wave propagation behavior of the random and the periodic composites becomes, once again, nearly identical; $\langle C_{1P}\rangle$ and $\langle C_{1R}\rangle$ agree within a few percent for all $n > 1.2$ MHz ($k_1a > 1.58$); the error in each measurement is 1%. There are a few gaps in the $\langle C_{1R}\rangle$ data, a discussion of the reasons for this is given in Section 4.6.

4.5 *Attenuation measurements*

In this paragraph we summarize some of the results concerning attenuation obtained by exact analysis of harmonic wave propagation through periodic *layered* composites with the direction of wave propagation *normal* to the layering[18–23]. These results provided the motivation for the attenuation measurements. By examining the Floquet waves, it has been shown independently by Lee and Yang[18] and by Delph *et al.*[22] that when the frequency belongs to a pass band (Brilloin zone), the wavenumber is real, i.e. $\langle \alpha_P\rangle = 0$. When the frequency belongs to a stop band, the wavenumber is purely imaginary, i.e. Floquet waves cannot be propagated. A lucid description of the associated physical events has been given by Lee[21]; here, for brevity, we will take this condition to mean that $\langle \alpha_P\rangle = \infty$. At the ends of the Brilloin zones ($\xi = m$) the wavenumber becomes complex, implying attenuated waves. Now there are two factors which distinguish the theory from the present experiments. One, the theories treat a laminated medium; the experiments are concerned with particulate composites. Two, it is difficult to estimate the extent to which Floquet waves (infinite wave in an infinite medium) are fully established in a laboratory specimen with a finite number of layers (modelling errors). Therefore, $\langle \alpha_P\rangle$ may be expected to be greater than zero at all frequencies due to energy scattered away from the direction of wave propagation, and due to matrix attenuation. The experiments were conducted with the expectation that $\langle \alpha_P\rangle$ will be relatively small in the pass bands and will go through rather sharp peaks in the stop bands. As will be seen, the measurements are significantly different from these expected results.

Turning to the case of *random* composites, the attenuation is expected to be greater than zero at all frequencies due to the fact that the incident wave is continuously scattered into incoherent waves[19].

The attention is first drawn to the $\langle \alpha_R\rangle$ curve in Fig. 6. This is characterized by a series of well defined peaks. The appearance of this curve is remarkably similar to the γ_N vs. k_1a curves for a single spherical scatterer, see Appendix H of[14]. Since the radius of the sphere, a, is the only characteristic dimension associated with a random composite, the existence of these peaks can only be attributed to the excitation of the particle resonances. (In [9] the average inter-particle distance was treated as a second characteristic dimension of the problem. However, it was found to have no influence on either $\langle C_1\rangle$ or $\langle \alpha\rangle$.) The frequency above which resonance effects become important is $n = 0.5$ MHz (approx.), i.e. $k_1a \leqq 0.7$. This is in good agreement with the analytical predictions where the first peak in γ_N appears around $k_1a = 0.5$

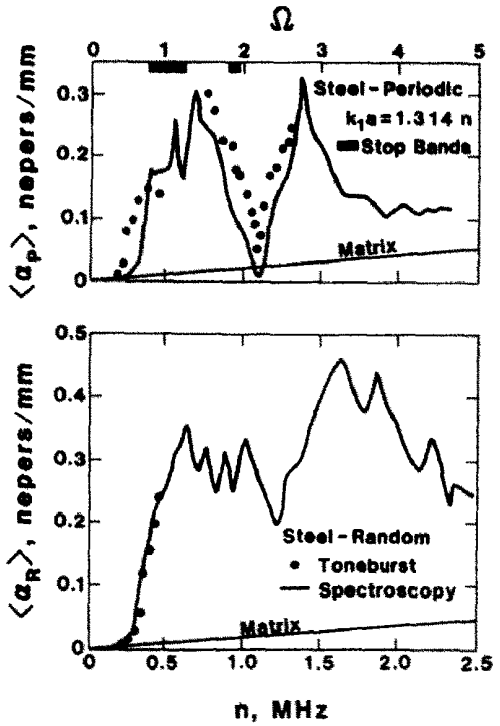

Fig. 6. Attenuation vs. Frequency in periodic (upper) and random (lower) steel/PMMA composites.

for a stainless steel sphere in magnesium[14] and an iron sphere in aluminum[13]. (Since γ_N vs k_1a results for steel/PMMA are not available in the literature, a direct comparison is not possible and the foregoing comparison is made only in an approximate sense.) It is well-known that at very low values of n(or k_1a), γ_N increases very rapidly with k_1a: as $(k_1a)^4$ in the Rayleigh limit; and as $(k_1a)^2$ at moderately small frequencies[19]. Some evidence of this is seen in the $\langle\alpha_R\rangle$ curve at low frequencies, $0 \leqq n \leqq 0.3$ MHz. In particular $\langle\alpha_R\rangle$ becomes immeasurably small below 0.2 MHz. For larger n, $0.3 \leqq n \leqq 0.6$ MHz or $0.4 \leqq k_1a \leqq 0.8$, $\langle\alpha_R\rangle$ may be seen to increase almost linearly with n. Finally, a comparison of $\langle\alpha_R\rangle$ in Fig. 6 with $\langle C_{1R}\rangle$ in Fig. 4 reveals that the attenuation is affected much more by particle resonance than is velocity.

Attention is now drawn to $\langle\alpha_P\rangle$ in Fig. 6. At low frequencies, $n < 0.4$ MHz, $\langle\alpha_P\rangle \cong \langle\alpha_R\rangle$. However, for $n > 0.4$ MHz (the first stop band is $0.37 < n < 0.6$ MHz), the similarity disappears. A general comparison of the two curves reveals the effect of lattice periodicity on $\langle\alpha_P\rangle$ (the particle resonance effects are common to both). Expectedly, $\langle\alpha_R\rangle$ is generally larger than $\langle\alpha_P\rangle$; this is particularly true at the high end of the frequency range where $\langle\alpha_P\rangle$ becomes small ($\cong$0.1 nepers/mm). The most remarkable feature, however, is that at about 1.1 MHz ($\Omega = 2.2$, third pass band, see Fig. 5) $\langle\alpha_P\rangle$ nearly vanishes (cf. $\langle\alpha_R\rangle = 0.25$ nepers/mm at the same frequency). Since this was a rather unexpected result, this data was checked repeatedly using the water-immersion apparatus as well as the direct-contact apparatus, and using the toneburst as well as the ultrasonic spectroscopy methods of measurement. Essentially the same results were obtained. For some inexplicable reason, the composite becomes nearly transparent at this particular frequency. A connection between the peaks of the attenuation curve and the stop band criterion, $\xi = m$, could not be established. This is probably because the $\langle\alpha_P\rangle$ curve is simultaneously recording the effect of lattice periodicity and the particle resonances. That $\langle\alpha_P\rangle$ could be measured continuously across the stop bands is due to the fact that ultrasonic spectroscopy could be used (see Section 3, Experimental Procedures). Note that even across the stop bands $\langle\alpha_P\rangle$ is not very large. Analytically, in a periodic *layered* composite, at cut-off, the incident wave is completely reflected, i.e. $\langle\alpha_P\rangle = \infty$. This brings out another important difference in the behavior of layered and particulate composites.

The attenuation data for the glass composite is shown in Fig. 7. The first peak occurs at 0.63 MHz ($k_1a = 1.56$, $\xi = 1.11$). This frequency is at the beginning of the first stop band; see Fig. 3.

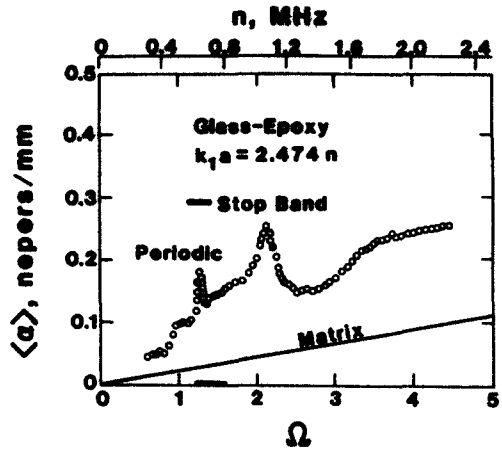

Fig. 7. Attenuation vs frequency in the periodic glass/epoxy composite.

However, the second peak occurs at 1.06 MHz and there is no jump in $\langle C_1 \rangle$ at that frequency. Furthermore, at the frequencies corresponding to the anticipated second and third stop bands, namely, 1.4 MHz ($\xi = 2$) and 2.0 MHz ($\xi = 3$), there are no peaks in the attenuation data. Therefore, as in the case of the steel composite, a connection between the attenuation peaks and the stop band criterion ($\xi = m$) cannot be established here as well.

4.6 *Time-domain data*

In this section the time-domain data for both the periodic and the random steel/PMMA composites is presented. The water immersion apparatus was used for Figs. 8(a–c); the direct contact apparatus was used for Figs. 8(d–g) and Figs. 9(a–d). In each oscillograph, the lower trace is the incident pulse (through water or through a block of polystyrene), the upper trace is the corresponding signal received through a composite. A critical requirement of the toneburst method is that, starting with the head of the pulse, one should be able to make an unequivocal one-to-one correspondence between the peaks of the incident and the refracted tonebursts. (In the following, for brevity, the word "correspondence" will be used to imply the preceding sentence.) When this correspondence breaks down, $\langle C_1 \rangle$ cannot be measured.

Periodic composites

First pass band ($0.17 \leqq n \leqq 0.37$ MHz). The frequency $n = 0.3$ MHz is arbitrarily selected as a typical frequency in the first pass band. Data traces are shown in Fig. 8(a). The one-to-one correspondence is obvious and $\langle C_1 \rangle$ could be measured.

First stop band ($0.37 < n < 0.6$ *MHz*). For $n = 0.5$ MHz ($\Omega = 1$), the traces are shown in Fig. 8(b). The incident toneburst (lower) has *six* "major" peaks aligned with graticules 2–7, the transmitted toneburst (upper) has *seven* major peaks in the same time interval. The "correspondence" breaks down and $\langle C_1 \rangle$ cannot be measured. Note also a severe harmonic distortion.

Second pass band ($0.6 \leqq n \leqq 0.9$ *MHz*). The traces at 0.67 MHz are shown in Fig. 8(c). Even though there is some distortion near the head of the pulse (which is to be expected for transient wave propagation through a highly dispersive medium) the "correspondence" is possible and $\langle C_1 \rangle$ could be measured.

Second stop band ($0.90 < n < 0.97$ *MHz*). Here, we have purposely selected a "border line" case: at 0.9 MHz, $\langle C_1 \rangle$ could be measured, at 0.91 MHz it could not, and the corresponding traces are shown in Fig. 8(d). The reasons are the same as in first stop band (see Fig. 8(b), 0.5 MHz). In particular, between the second and the eighth graticule inclusive, there are *twelve* and *fourteen* peaks in the incident and the transmitted waveform, respectively.

Third pass band ($0.97 \leqq n \leqq 2.3$ *MHz*). The traces at 1.18 MHz are shown in Fig. 8(e). The remarks concerning the second pass band (0.67 MHz, Fig. 8c) also apply here.

(*Anticipated*) *third and fourth stop bands.* In Section 4.2 it was mentioned that two higher stop bands anticipated at 1.5 MHz ($\xi = 3$) and 1.9 MHz ($\xi = 4$) were not observed; instead, $\langle C_1 \rangle$

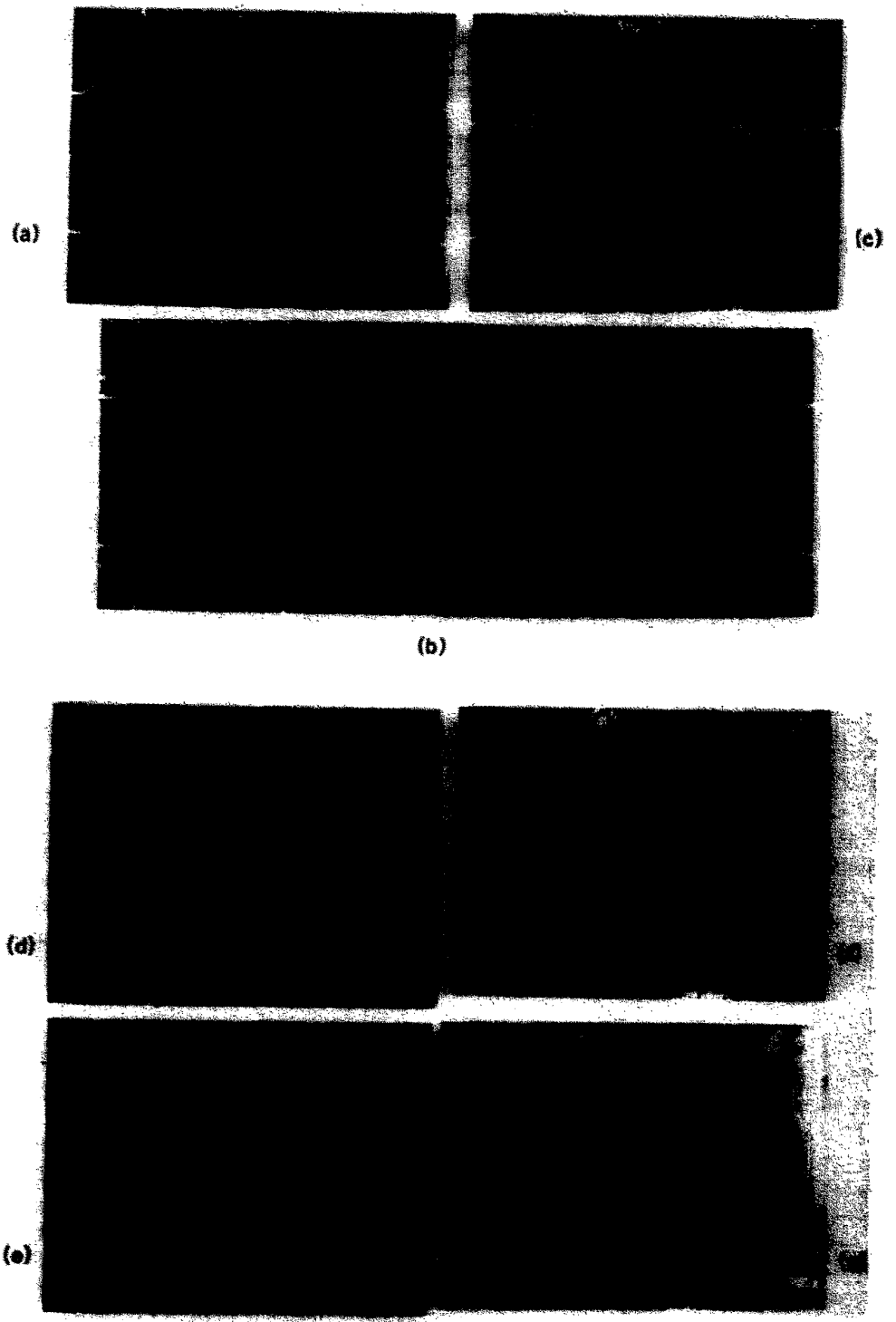

Fig. 8. Time domain data for the periodic steel/PMMA composite. Lower: incident wave. Upper: transmitted wave. (a) First pass band. $n = 0.3$ MHz, $\xi = 0.91$. (b) First stop band. $n = 0.5$ MHz. (c) Second pass band. $n = 0.67$ MHz, $\xi = 1.37$. (d) Second stop band. $n = 0.91$ MHz. (e) Third pass band. $n = 1.18$ MHz, $\xi = 2.15$. (f) Third stop band, anticipated at $n = 1.5$ MHz, $\xi = 3$ was not observed. (g) Fourth stop band, anticipated at $n = 2.0$ MHz, $\xi = 4$ was not observed.

varied continuously across these frequencies (see Figs. 4 and 5). The time-domain data at 1.5 and 2.0 MHz are shown in Figs. 8(f, g), respectively. In Fig. 8(f), the transmitted wave does take a long period of time before steady state is established, however, there is no difficulty in establishing the "correspondence". The reference peak was chosen somewhere past the twentieth peak. The same remarks apply to Fig. 8(g).

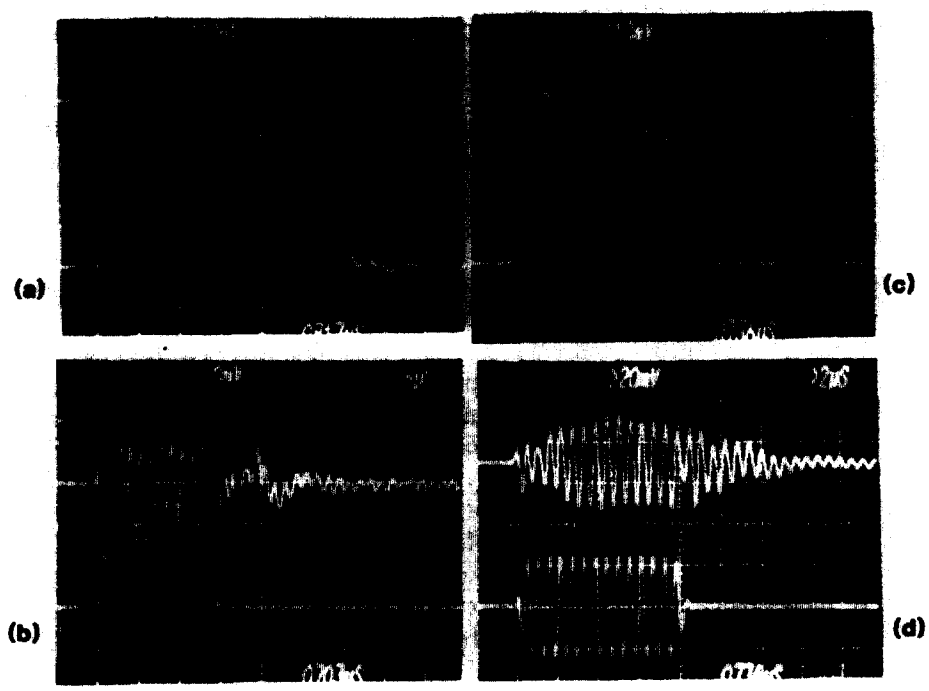

Fig. 9. Time domain data for the random steel/PMMA composite. Lower: Incident wave. Upper: Transmitted wave. (a) $n = 0.3$ MHz, $k_1 a = 0.39$ (Long-wavelength regime). (b) $n = 0.8$ MHz, $k_1 a = 1.05$. (c) $n = 0.9$ MHz, $k_1 a = 1.18$. $\langle C_1 \rangle$ cannot be measured. (d) $n = 1.05$ MHz, $k_1 a = 1.38$. $\langle C_1 \rangle$ can be measured.

We now point to another interesting phenomenon in periodic particulate composites. With reference to Figs. 8(b, c, e), note that that the composite continues to oscillate (much like an underdamped oscillator) long after the excitation signal stops. Also in Figs. 8(c, e), the composite takes several cycles before it builds up to its steady state amplitude. This phenomenon occurred to varying degrees at all frequencies tested. These phenomena strongly indicate that there is some mechanism of storing energy in the composite. When the toneburst strikes the quiescent composite, energy is extracted from the toneburst (hence a gradual build-up of amplitude); once toneburst leaves the composite, the stored energy is slowly leaked back into the propagating wave (hence a gradual amplitude decay). Now, Lee and Yang[18], in their work with passage of Floquet waves in periodic *layered* composites, have shown that at the ends of a stop band, the wave motion can be interpreted in terms of the normal modes of oscillations of a unit cell. It appears that these normal modes provide the necessary mechanism for energy storage.

Random composites

The time-domain data for the steel/PMMA composite are shown in Fig. 9. In Fig. 9(a), $n = 0.3$ MHz, $k_1 a = 0.39 < 1$, i.e. this frequency belongs to the long-wavelength regime. The "correspondence" is obvious. Note that unlike the periodic composite, here the transmitted pulse decays rapidly after the excitation stops. The data at $n = 0.8$ MHz, $k_1 a = 1.05$ are shown in Fig. 9(b). Although there is a slight distortion, it is still possible to measure $\langle C_1 \rangle$. However, at 0.9 MHz ($k_1 a = 1.18$, Fig. 9c) it is no longer possible to measure $\langle C_1 \rangle$ due to severe distortion of the transmitted wave: this is the reason for the gaps in $\langle C_{1R} \rangle$ in Fig. 4. In Fig. 9(d), $n = 1.05$ MHz ($k_1 a = 1.38$) $\langle C_1 \rangle$ can, once again, be measured. Note that the oscillations of the composite after the excitation signal stops continue to increase in amplitude as $k_1 a$ increases. For the case of periodic composites, this phenomenon was attributed to the normal modes of oscillations of a unit cell. For the case of random composites, it is attributed to the normal modes of vibrations of the spherical inclusions.

Finally, the numerical values of the data presented in this paper are included in the Appendix.

5. DISCUSSION

In the preceding section a number of important differences in the mechanical behavior of periodic layered and periodic particulate composites were noted. In this section we include a brief discussion to put these differences in a perspective. Consider a plane P-wave incident upon a (one-dimensional) layered composite. Both the reflection and the refraction of this wave at each of the interfaces will be a plane longitudinal wave. Now consider the same wave incident upon a (three-dimensional) particulate composite. The scattered field is neither plane nor only longitudinal; it consists of both P- and S-waves propagated along spherical wavefronts.

Next, consider the stop bands ($\xi = m$) of a layered composite. Lee and Yang[18] have shown that the wave motion can be interpreted in terms of the normal modes of oscillation of a unit cell, there is no propagation, and the group velocity is zero. It is easy to show that this is not true for a periodic particulate composite. Consider the case when the incident wavelength is very small compared to both a and d (often called the optical limit). For the present case of a stiff inclusion in a compliant matrix, the cross-sectional area occupied by the spheres is essentially opaque to the incident wave, the remainder of the area is essentially transparent. Due to periodicity, the spheres in the interior of the composite lie in the shadow of the spheres in the first layer. Hence, there exists a bundle of rays along the symmetry axis such that the ray does not intersect any of the (acoustically opaque) inclusions, i.e. it lies entirely in the (acoustically transparent) matrix. Therefore, even when the stop-band condition, $\xi = m$, is satisfied there will be some energy propagated from a transmitter to a receiver cemented to the two faces of the composite along this bundle of rays. Therefore, the *group velocity* will not be zero.

Finally, the resonance of a particle, which is a three-dimensional phenomenon, has no direct equivalence in the layered composite.

6. CONCLUSIONS

An important property of the periodic heterogeneous materials is the phenomenon of pass bands and stop bands. This phenomenon has been experimentally studied for the case of periodic *particulate* (i.e. three-dimensional) composites. Two pass bands and one stop band were observed for the glass/epoxy composite, whereas three pass bands and two stop bands were found for the steel/PMMA case. Along the frequency axis, as a stop band is approached from left, the phase velocity decreases; conversely, as the stop band is approached from right, the velocity increases; across the stop band, velocity takes a large positive jump with increasing frequency. In both composites, at higher frequencies where the wavelength becomes comparable to the radius of the spherical inclusion ($k_1 a > 1$), the higher stop bands are not observed and the dispersion curve becomes continuous; this is a rather surprising result of the present experiments. We have conjectured that this is probably due to the excitation of resonances of the spherical inclusions which, at higher frequencies, tend to dominate the resonances of the unit cell. Another surprising result is that unlike the case of layered (one-dimensional) periodic composites, the pass bands for a particulate composite *overlap* along the wave number axis.

Acknowledgements—Thanks are due to Karl Rupp for his help in designing and fabricating the two ultrasonic apparatuses, to M. S. Petraitis for preparing the glass/epoxy composite, to Karl Rupp, Rich Cowgill, and Mike Hacker for their prompt and excellent technical assistance through the course of this investigation, and to Carol Osborne for her patience and care in preparing the manuscript. We would also like to thank one of the referees for making several helpful suggestions.

The financial support of the National Science Foundation under grant ENG 78-10168 to the University of Colorado at Boulder is gratefully acknowledged.

A minor part of this work was supported by a grant from the Council on Creative and Research Work of the University of Colorado, Boulder.

REFERENCES

1. A. Bedford, D. S. Drumheller and H. J. Sutherland, On modeling the dynamics of composite materials. *Mechanics Today* **3**, 1–54 (1976).
2. E. H. Lee (ed.), *Dynamics of Composite Materials*. New York (1972).
3. C. W. Robinson and G. W. Leppelmeir, Experimental verification of dispersion relations for layered composites. *J. Appl. Mech.* **41**, 89–91 (1976).

4. J. S. Whittier and J. C. Peck, Experiments on dispersive pulse propagation in laminated composites and comparison with theory. *J. Appl. Mech.* **36**, 485–490 (1969).
5. H. J. Sutherland and R. Lingle, Geometric dispersion of acoustic waves by a fibrous composite. *J. Composite Materials* **6**, 490–502 (1972).
6. T. R. Tauchert and A. N. Guzelsu, An experimental study of dispersion of stress waves in a fiber-reinforced composite. *J. Appl. Mech.* **39**, 98–102 (1972).
7. TRA-CAST 3012 epoxy. TRA-CON Inc., Resin Systems Division, 55 North Street, Medford, Ma 02155. (617) 391-5540. It is a low viscosity 100% solids (no solvents) epoxy resin and hardener system. Mixing proportions: 46 parts hardener, 100 parts resin by weight. After mixing thoroughly, the solution was placed in a vacuum chamber until all air was evacuated. The epoxy was then cured at 65°C for 24 hr.
8. Buehler Transoptic Powder. Buehler Ltd., 2120 Greenwood Street, Evanston, IL 60204.
9. V. K. Kinra, M. S. Petraitis and S. K. Datta, Ultrasonic wave propagation in a random particulate composite. *Int. J. Solids Structures* **16**, 301–312 (1980).
10. Panametrics, Inc., 221 Crescent Street, Waltham, MA 02154, (617) 899–2719. Automation Industries, Inc., Sperry Division, Shelter Rock Road, Danbury, CT 06510, (203) 748–3581.
11. Valpey-Fisher, Inc., 75 South Street, Hopkinton, MA 01748.
12. Hartforld Ball Company, Rocky Hill, CT 06067, (203) 563-0111.
13. L. Flax and H. Überall, Resonant scattering of elastic waves from spherical solid inclusions. *J. Acous. Soc. Am.* **47**(5), 1432–1442 (1980).
14. R. Truell, C. Elbaum and B. B. Chick, *Ultrasonic Methods in Solid State Physics.* Academic Press, New York (1969).
15. V. K. Kinra, E. Ker and S. K. Datta, Influence of particle resonance on wave propagation in a random particulate composite. *Mech. Res. Commun.* **9**, 109–114 (1982).
16. S. K. Datta, Scattering by a random distribution of inclusions and effective elastic properties. *Continuum Model of Discrete Systems* (Edited by J. W. Provan), pp. 111–127. Univ. of Waterloo Press (1978).
17. V. K. Kinra and A. Anand, Wave propagation in a random particulate composite at long and short wavelengths. *Int. J. Solids Structures* **8**, 367–380 (1982).
18. E. H. Lee and Wei H. Yang, On waves in composite materials with periodic structure. *SIAM J. Appl. Math.* **25**, 492–499 (1973).
19. R. M. Christensen, Wave propagation in layered elastic media. *J. Appl. Mech.* **42**, 153–158 (1975).
20. Sargent Welch Scientific, P.O.B. 7196, Denver, Colorado 80207.
21. E. H. Lee, Wave propagation in composites with periodic structures. *Fifth Canadian Congress of Applied Mathematics*, pp. G49–G59 (1975).
22. T. J. Delph, G. Herrmann and R. K. Kaul, Harmonic wave propagation in a periodically layered, infinite elastic body: plane strain, analytical results. *ASME J. Appl. Mech.* **46**, 113–119 (1979).
23. G. Herrmann, R. K. Kaul and T. J. Delph, On continuum modelling of the dynamic behavior of layered composites. *Archiv. Mech.* **28**, 405–421, Warsaw (1976).
24. B. Q. Vu and V. K. Kinra, Diffraction of Rayleigh waves in a half-space. Rep. CUMER-81-7, Department of Mechanical Engineering, University of Colorado, Boulder, CO 80309 1981.
25. V. K. Kinra and E. L. Ker, Effective elastic moduli of a thin-walled glass microsphere/PMMA composite. *J. Composite Materials* **16**, 117–138 (1982).
26. B. Hartmann and J. Jarzynski, Immersion apparatus for ultrasonic measurements in polymers. *J. Acous. Soc. Am.* **56**, 1469–1477 (1974).
27. B. Hartmann and J. Jarzynski, Ultrasonic hysteresis absorption in polymers. *J. Appl. Phys.* **43**, 4304–3212 (1972).
28. V. K. Kinra and A. Anand, Dynamic behavior of random particulate composites at ultrasonic frequencies. CUMER 80-6, Department of Mechanical Engineering, University of Colorado, Boulder (1980).
29. F. C. Moon and C. C. Mow, Wave propagation in a composite material containing dispersed rigid spherical inclusions. The Rand Comporation Rep. RM-6139-PR, Rand, 1700 Main Street, Santa Monica, CA 90406.

APPENDIX
Numerical values of data*

1. Glass/Epoxy Periodic Composite

n	$\langle C_l \rangle / C_l$	n	$\langle \alpha_p \rangle$	n (continued)	$\langle \alpha_p \rangle$ (continued)
0.296	1.30	0.300	0.05	1.100	0.26
0.350	1.27	0.325	0.05	1.125	0.21
0.408	1.23	0.351	0.05	1.154	0.20
0.457	1.19	0.375	0.05	1.175	0.17
0.507	1.18	0.400	0.05	1.174	0.16
0.557	1.18	0.425	0.06	1.203	0.16
0.580	1.15	0.450	0.08	1.252	0.15
0.601	1.14	0.476	0.10	1.272	0.15
0.807	1.45	0.486	0.10	1.301	0.15
0.833	1.46	0.500	0.10	1.330	0.15
0.858	1.45	0.526	0.10	1.364	0.15
0.906	1.43	0.550	0.10	1.400	0.15
0.958	1.41	0.573	0.10	1.430	0.20
1.003	1.41	0.600	0.12	1.472	0.20
1.101	1.41	0.625	0.18	1.510	0.19
1.200	1.39	0.635	0.15	1.539	0.20
1.304	1.38	0.650	0.13	1.603	0.20
1.400	1.39	0.671	0.13	1.630	0.20
1.502	1.38	0.700	0.14	1.664	0.21
1.552	1.36	0.725	0.14	1.703	0.22
1.606	1.35	0.751	0.15	1.747	0.23
1.706	1.34	0.775	0.15	1.773	0.23
1.851	1.33	0.800	0.16	1.815	0.23
1.903	1.33	0.826	0.18	1.834	0.24
1.952	1.33	0.876	0.18	1.870	0.23
2.000	1.34	0.900	0.19	1.908	0.24
2.051	1.33	0.925	0.19	1.932	0.24
		0.956	0.18	1.970	0.24
		0.975	0.19	2.006	0.24
		1.000	0.22	2.037	0.24
		1.026	0.22	2.074	0.24
		1.050	0.21	2.103	0.24
		1.076	0.23	2.139	0.25
				2.176	0.25

2. Steel/PMMA Composites

n	$\langle \alpha_R \rangle$	$\langle \alpha_p \rangle$	n	$\langle C_l \rangle / C_l$ Random	$\langle C_l \rangle / C_l$ Periodic	n	$\langle C_l \rangle / C_l$ Random	$\langle C_l \rangle / C_l$ Periodic
0.170	0.003	0.011	0.170	0.84	0.76	1.200	1.09	1.09
0.200	0.006	0.025	0.200	0.84	0.74	1.235	1.08	1.07
0.235	0.022	0.077	0.235	0.83	0.73	1.270	1.08	1.07
0.270	0.033	0.086	0.270	0.83	0.73	1.300	1.07	1.06
0.300	0.058	0.130	0.300	0.83	0.63	1.335	1.08	1.05
0.335	0.123	0.135	0.335	0.84	0.59	1.370	1.07	1.04
0.370	0.157	0.122	0.370	0.84	0.56	1.400	1.06	1.03
0.400	0.201	0.120	0.400	0.84	-	1.435	1.05	1.02
0.430	0.245	-	0.430	0.86	-	1.470	1.05	1.01
0.770	-	0.29	0.470	0.90	-	1.500	1.04	1.01
0.800		0.27	0.500	0.93	-	1.550	1.04	1.01
0.835		0.24	0.535	0.95	-	1.600	1.03	1.01
0.900		0.24	0.570	0.93	-	1.700	1.03	1.01
0.970		0.20	0.600	0.93	1.09	1.750	1.02	1.02
1.000		0.15	0.635	0.93	1.03	1.800	1.02	1.02
1.035		0.14	0.670	0.94	0.98	1.850	1.01	1.01
1.070		0.06	0.700	0.96	0.96	1.900	1.01	1.00
1.100		0.07	0.735	0.94	0.94	1.950	1.01	1.00
1.135		0.12	0.770	0.94	0.91	2.000	1.00	1.00
1.170		0.17	0.800	0.93	0.88	2.050	1.00	0.99
1.200		0.18	0.835	0.94	0.86	2.100	1.00	1.00
1.235		0.19	0.870	0.94	0.82	2.150	1.00	0.97
1.270		0.22	0.900	JUMP	0.77	2.200	1.00	0.97
1.300		0.24	0.970	1.05	1.28	2.250	1.00	0.96
			1.000	1.04	1.23	2.300	1.00	0.96
			1.035	1.03	1.19			
			1.070	1.02	1.17			
			1.100	1.02	1.14			
			1.135	1.01	1.12			
			1.170	JUMP	1.11			

*Frequency n in MHz, attenuation $\langle \alpha \rangle$ in nepers/mm.